J Appl Electrochem (2009) 39:1385–1392
DOI 10.1007/s10800-009-9814-5

ORIGINAL PAPER

Effects of minor additions of ruthenium on the passivation of duplex stainless-steel corrosion in concentrated hydrochloric acid solutions

El-Sayed M. Sherif · J. H. Potgieter · J. D. Comins · L. Cornish · P. A. Olubambi · C. N. Machio

Received: 24 October 2008 / Accepted: 26 January 2009 / Published online: 14 February 2009

Abstract The effects of minor additions of ruthenium (0.14%, 0.22%, and 0.28%) on the passivation of duplex stainless-steel (DSS, Fe–22%Cr–9%Ni–3%Mo) corrosion in 2 M HCl solutions have been studied using open-circuit potential (OCP), potentiodynamic cyclic polarization, potentiostatic current–time, electrochemical impedance spectroscopy (EIS), and weight loss measurements. OCP measurements showed an increased shift in the corrosion potential to more positive values with increasing Ru content. Polarization and EIS experiments indicated that the presence of Ru and the increase of its content decrease the corrosion rate, critical and passive current density, and polarization resistance. Moreover, it shifts the corrosion and pitting potentials to more positive values. Current–time measurements at −100, −50, and 50 mV versus Ag/AgCl also confirmed that the severity of pitting corrosion decreases with an increasing Ru content. Weight-loss time data showed good agreement with the electrochemical measurements.

Keywords Concentrated hydrochloric acid solutions · Corrosion passivation · Duplex stainless-steel · Ruthenium additions

1 Introduction

It is well known that the corrosion resistance of virtually all stainless-steels can be remarkably increased by alloying them with minor additions of platinum group metals (PGMs) [1, 2]. Sufficient amounts of these alloying components not only retard the anodic dissolution of steels to which they are added but also increase the effectiveness of cathodic processes owing to the reduced overvoltage of hydrogen on them [3–5]. The fact that ruthenium is the cheapest of the PGMs perpetuates the interest in the spontaneous passivation processes of steels containing small amounts of Ru as alloying component [6–10]. Potgieter et al. [11] have studied the effect of minor additions of Ru on the passivation of duplex stainless-steels (DSSs) in 40% H_2SO_4 and found that the presence of Ru inhibits the anodic dissolution behavior when active corrosion takes place. It has also been reported [6] that the presence of Ru in the DSS alloy increases the formation of Cr_2O_3 and Fe_3O_4 in the passive film, compared to normal DSS that contained no Ru. These observations correlate with the fact that Ru acts as a blocking agent, which decreases the

E.-S. M. Sherif · J. D. Comins
DST/NRF Center of Excellence in Strong Materials, School of Physics, University of the Witwatersrand, Wits 2050, Johannesburg, South Africa

J. H. Potgieter
Chemistry and Materials Division, School of Biology, Chemistry and Health Sciences, Manchester Metropolitan University, Oxford Road, Manchester M1 5GD, UK

L. Cornish · P. A. Olubambi · C. N. Machio
DST/NRF Center of Excellence in Strong Materials, School of Chemical and Metallurgical Engineering, University of the Witwatersrand, Wits 2050, Johannesburg, South Africa

E.-S. M. Sherif
Center of Excellence for Research in Engineering Materials (CEREM), College of Engineering, King Saud University, P.O. Box 800, Al-Riyadh 11421, Saudi Arabia

E.-S. M. Sherif (✉)
Physical Chemistry Department, National Research Centre, Dokki, Cairo, Egypt
e-mail: esherif@ksu.edu.sa; emsherif@gmail.com

dissolution rates of Cr and Fe, and therefore increases the probability to form a stable passive layer.

The present work reports the effects of minor Ru additions on the passivation of DSS corrosion in 2 M HCl solution. The presence of Ru in DSS was expected to improve the corrosion resistance of the alloy as a result of the ability of Ru to inhibit the anodic reactions as well as modify the efficiency of the cathodic process of the alloy. Particular attention was paid to the effect of Ru on the pitting corrosion of DSS, which has, to date, received little attention. The investigation was carried out using open-circuit potential (OCP), potentiodynamic cyclic polarization, potentiostatic current–time, EIS, and weight-loss measurements.

2 Experimental procedure

2.1 Materials and electrochemical cell

Hydrochloric acid (HCl, Merck, 32%), was used as received. The alloys used in this study were DSSs with a nominal composition of Fe–22%Cr–9%Ni–3%Mo containing 0% (alloy I), 0.14% (alloy II), 0.22% (alloy III), and 0.28% Ru (alloy IV), respectively, and having rectangular dimensions of 1 × 1 × 0.4 cm, with total exposed area of 1 cm^2. An electrochemical cell with a three-electrode configuration was used; the DSS alloys, a platinum foil, and an Ag/AgCl electrode (in 3 M KCl) were used as working, counter, and reference electrodes, respectively. The DSS electrodes were first polished successively with metallographic emery paper of increasing fineness of up to 1,000 grit then washed with doubly distilled water, degreased with acetone, washed using doubly distilled water again and finally dried with tissue paper.

2.2 Electrochemical methods

Electrochemical experiments were performed by using a PARC Parstat-2273 Advanced Electrochemical System. For potentiodynamic cyclic polarization experiments, the potential was started at −800 mV and swept in the positive direction up to 1,000 mV at a scan rate of 3 mV/s. Potentiostatic current–time experiments were carried out by setting the potential at −100, −50, and 50 mV versus Ag/AgCl for 1,500 s. Impedance (EIS) tests were performed at corrosion potentials (E_{Corr}) after 1 h of the alloy immersion in the test electrolyte over a frequency range of 100 KHz to 0.05 Hz, with an ac wave of ±5 mV peak-to-peak overlaid on a dc bias potential. The impedance data were collected using Powersine software at a rate of ten points per decade change in frequency.

2.3 Weight-loss measurements

The weight-loss experiments were carried out using cylindrical DSS coupons having dimensions of 1.5 cm diameter and 0.3 cm height with a total exposed area of 4.95 cm^2. The coupons were polished and dried in the same way as the DSS electrodes were, weighed (W_1), and then suspended in 200 cm^3 solutions of 2 M HCl for different exposure periods (6–48 h). At the end of a run, the samples were rinsed with distilled water, cleaned with acetone, dried, and then weighed again (W_2). All weight-loss measurements were performed in triplicate and the maximum standard deviation in the observed weight loss was ±1.5%.

3 Results and discussion

3.1 Open-circuit potential measurements

The OCP curves of the DSS alloy I (1), alloy II (2), alloy III (3) and alloy IV (4) in 2 M HCl solutions are shown in Fig. 1. It can clearly be seen from Fig. 1 that the acid solution increased the potential of alloy I (curve 1) to the more negative values in the first few moments, which could be due to the dissolution of the oxide film formed on the alloy surface in air before its immersion into the test solution. Increasing the immersion time led to a rapid positive shift in the potential of the alloy, possibly due to the chemical reaction between the acid molecules and the surface. This positive shift in the potential continued to occur rapidly over the first 4 h, after which the potential started to increase slightly in the same positive direction until the end of the experiment. This can be attributed to the formation of an oxide film and/or some corrosion

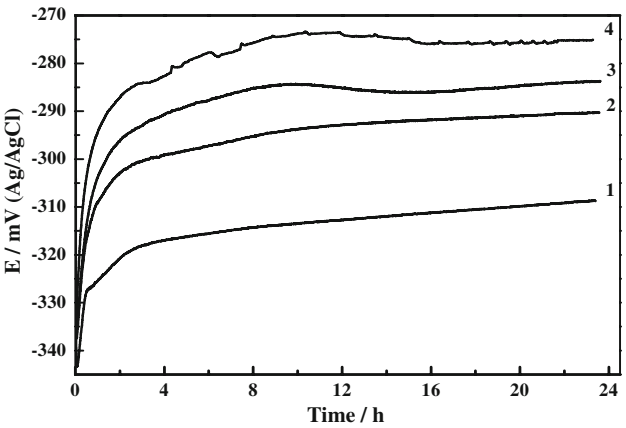

Fig. 1 Variations of the open-circuit potential with time for the duplex stainless-steel, alloy I (1), alloy II (2), alloy III (3), and alloy IV (4) in 2 M HCl solution

products that protected the surface of the alloy. The addition of 0.14% Ru in alloy II (curve 2) caused it to show nearly the same behavior as alloy I, with a higher positive potential shift during the running time of the experiment. Further positive potential shifts were recorded with increasing the Ru content to 0.22% (alloy III, curve 3) and 0.28% (alloy IV, curve 4). The recorded OCP was about ~ -310 mV for alloy I after 24 h of immersion. This value increased to ~ -290, -284, and -275 mV when the Ru content was increased from 0.14% to 0.22% and 0.28%, respectively. This indicates that the presence of Ru increases the corrosion resistance of the DSS alloy. This agrees with previous work [1, 5, 6], in which it was reported that stainless-steels with Ru as minor alloying component are passivated spontaneously due to the formation of passive layers of remarkably increased corrosion resistance on their surfaces, that shifted the corrosion potential of these alloys toward the more positive values.

3.2 Potentiodynamic cyclic polarization

The potentiodynamic cyclic polarization curves for alloy I (a), alloy II (b), alloy III (c) and alloy IV (d) in 2 M HCl solution are shown in Fig. 2. It is generally believed that the anodic reaction of steel in acidic solutions is the dissolution of iron,

$$Fe \rightarrow Fe^{2+} + 2e^{-} \quad (1)$$

The electrons produced by this reaction are consumed at the cathode due to the hydrogen ion reduction, which is the predominant cathodic reaction,

$$2H^{+} + 2e^{-} \rightarrow H_2 \quad (2)$$

The anodic branch for the DSS alloy I (Fig. 2a) shows an active–passive region. The active region is probably due to the dissolution of iron as shown in reaction (1). The passive region starts from the critical potential (E_{Crit}), at which the current reaches its maximum value (critical current, j_{Crit}). The current then decreases to show a large passive area with increasing potential due to the formation of oxide layers and/or corrosion products on the alloy surface. Increasing the potential in the more positive direction results in a complete dissolution and breakdown of the formed passive film, which could have led to the rapid increase of current on the curve. Reversing the potential in the backward direction showed higher currents than those of the forward ones due to the occurrence of pitting corrosion at potentials $\geq$ the pitting potential (E_{Pit}) and currents $\geq$ the pitting current (j_{Pit}).

The presence of Ru and the increase of its content in the DSS alloy (Fig. 2, panels b–d) significantly decreased the cathodic, corrosion (j_{Corr}), anodic, and j_{Crit} currents as well as shifting the corrosion (E_{Corr}), E_{Crit}, and E_{Pit} potentials to more positive values. A relative decrease can be seen in the

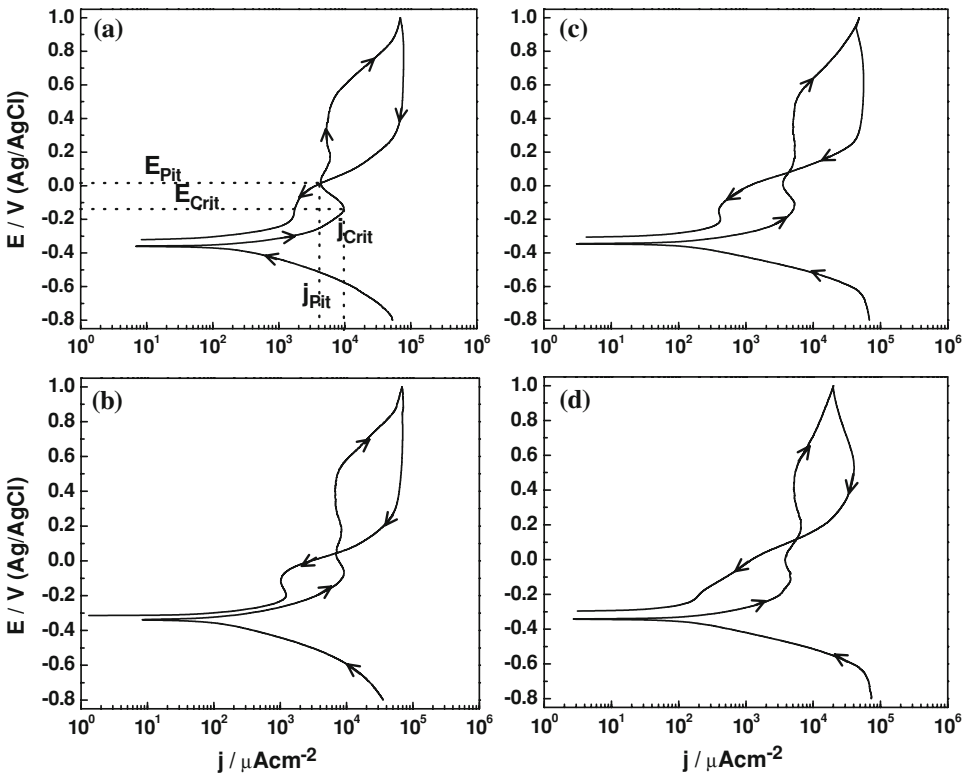

Fig. 2 Potentiodynamic cyclic polarization curves for **a** alloy I, **b** alloy II, **c** alloy III, and **d** alloy IV in 2 M HCl solutions

Table 1 Corrosion parameters obtained from potentiodynamic cyclic polarization curves shown in Fig. 2 for the DSS alloys in 2 M HCl solution

Alloy	Parameter										
	β_c (mV dec^{-1})	E_{Corr} (mV)	j_{Corr} (μA cm^{-2})	β_a (mV dec^{-1})	E_{Crit} (mV)	j_{Crit} (μA cm^{-2})	E_{Pit} (mV)	j_{Pit} (μA cm^{-2})	R_P (Ω cm^2)	K_{Corr} (mm year^{-1})	PE (%)
I	70	−370	400	100	−138	969	15	4,200	0.045	4.01	–
II	80	−345	149	105	−62	916	45	5,500	0.13	1.49	62.74
III	88	−340	73	112	−113	533	75	6,200	0.29	0.73	81.75
IV	95	−338	51	120	−80	470	120	7,000	0.45	0.50	87.52

area of the hysteresis loop of the polarization curves. The values of the cathodic (β_c) and anodic (β_a) Tafel slopes, j_{Corr}, E_{Corr}, j_{Crit}, j_{Pit}, E_{Crit}, E_{Pit}, polarization resistance (R_P), corrosion rate (K_{Corr}), and percentage of the passivation efficiency (PE%) obtained from Fig. 2 are listed in Table 1. The values of j_{Corr} and E_{Corr} were obtained from the extrapolation of anodic and cathodic Tafel lines located next to the linearized current regions [12–16]. The R_P and K_{Corr} values were also calculated as reported in our previous studies [12–16]. The values of PE% were obtained as in the case of the inhibition efficiency as follows [17, 18],

$$\mathrm{PE}\% = \frac{j^1_{Corr} - j^2_{Corr}}{j^1_{Corr}} \times 100 \quad (3)$$

Here j^1_{Corr} and j^2_{Corr} are the corrosion currents for the DSS alloys in the absence and presence of Ru, respectively.

The decreases in cathodic, corrosion (j_{Corr}), anodic, and j_{Crit} currents and K_{Corr} as well as the increases in j_{Pit}, R_P, and PE% with the presence of an increasing Ru content are mainly due to the increased surface resistance of the DSS against general and pitting attacks. The positive shifts in the E_{Corr}, E_{Crit}, and E_{Pit} and also the increases in the β_c and β_a values are apparently due to decreasing the general dissolution and pitting corrosion of the alloy through decreasing the rate of the anodic and cathodic reactions [4, 5]. This indicates that the presence of Ru, and its increasing content, enhance the passivation parameters on the DSS surface against corrosion. This might be due to the role of Ru in the formation of a thin, compact film on the alloy surface [10, 19]. It has also reported [5, 10, 20] that the presence of Ru in the DSS alloy leads to a possible Ru interaction effect with Fe that leads to the formation of Fe_3O_4 and allows the free diffusion of Cr to the surface to form Cr_2O_3, which could decrease the general and pitting corrosion of the DSS alloy as have been seen from Fig. 2 and the values in Table 1.

3.3 Potentiostatic current–time measurements

In order to shed more light on the effect of Ru additions on the passivation of DSS alloy and its ability to reduce the severity of pitting corrosion, potentiostatic current–time experiments at constant potential values [−100 mV (active region), −50 mV (transpassive region), and 50 mV (passive region)] were carried out. These potential values were chosen from the polarization curves shown in Fig. 2. The variation of the dissolution currents of alloy I (1), alloy II (2), alloy III (3), and alloy IV (4) as a function of time at −100 mV (a), −50 mV (b), and 50 mV (c) versus Ag/AgCl in 2 M HCl solution are shown in Fig. 3. It is clear from Fig. 3a (curve 1) that the current for alloy I increased rapidly in the first few seconds to reach its maximum after 500 s, which might be due to the dissolution of the alloy surface and probable pitting corrosion initiation. The pits no longer propagated and the current decreased slightly with time till the end of the run as a result of the formation of corrosion products that partially protect the surface. The addition of 0.14% Ru (curve 2) results in a decrease of current during alloy immersion and polarization. Increasing the Ru content to 0.22% and 0.28% (curves 3 and 4) shows the same current time behavior than for alloy II with lower absolute currents. This indicates that the DSS alloy does not suffer pitting corrosion at −100 mV and the addition of increasing amounts of Ru improve the corrosion resistance of the alloy.

Increasing the applied potential to −50 mV, as illustrated in Fig. 3b, resulted in a decrease of the absolute currents for the DSS alloy in comparison to those obtained at −100 mV (Fig. 3a). This can be explained by considering the polarization curves, where it is illustrated that −50 mV lies in the passivation potential range of the alloy, but −100 mV is in the active region. The presence of Ru and the increase of its content provided further decreases in the current values with time. On the other hand, stepping the potential to 50 mV (Fig. 3c) showed a higher current value for alloy I. This value decreased rapidly in the first few seconds before recording higher increases again with time. The initial decrease resulted from the formation of a passive layer, which was not protective enough, and therefore an increase of current with time occurred due to the breakdown of the passive layer and the occurrence of pitting corrosion [21]. The presence of Ru in alloys II and

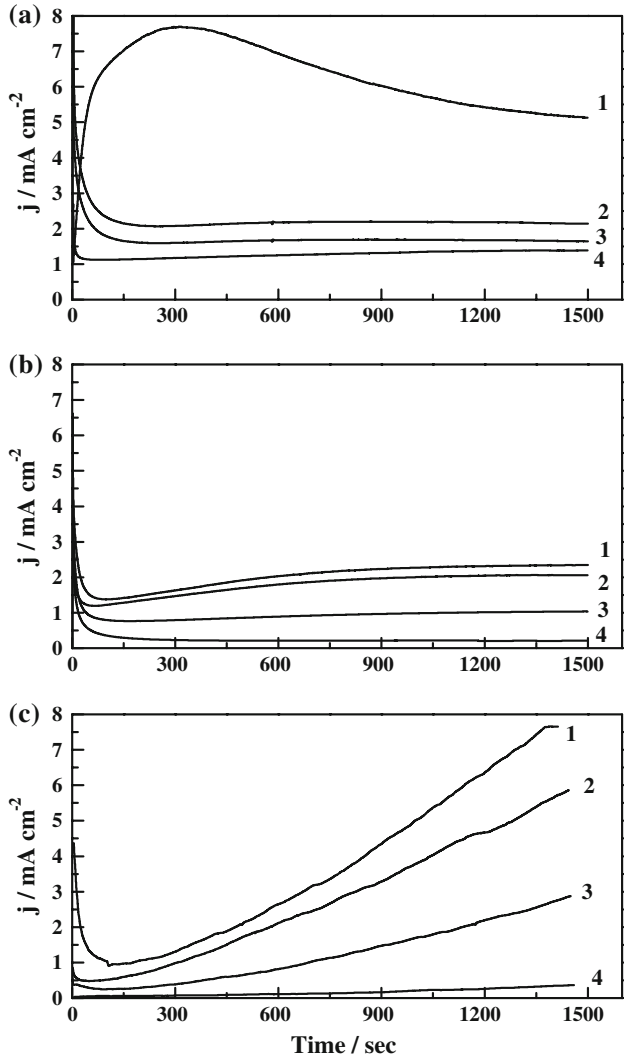

Fig. 3 Potentiostatic current time measurements for (1) alloy I, (2) alloy II, (3) alloy III, and (4) alloy IV in 2 M HCl solution at −100 (**a**), −50 (**b**) and 50 mV (**c**) versus Ag/AgCl

III, showed almost the same behavior with lower current values over the exposure time. This indicates a reduced severity of pitting corrosion of the alloy with the presence of increasing Ru amounts. This effect was confirmed with the presence of 0.28% Ru (alloy IV), which provided the minimum current values and a greatly suppressed pitting corrosion. This also agrees with the polarization data and confirms the ability of the increased amounts of Ru to passivate the alloy against general corrosion and prevent pitting attack.

3.4 Electrochemical impedance spectroscopy measurements

The electrochemical impedance spectroscopy (EIS) provides important mechanistic and kinetic information for electrochemical systems under investigation [22, 23]. The method was previously successfully employed to explain the corrosion and corrosion inhibition of metals in chloride media [24–28]. Figure 4 shows the Nyquist (a), Bode (b), and phase angle (c) plots for DSS alloy I (1), alloy II (2), alloy III (3), and alloy IV (4), respectively after 1 h immersion in 2 M HCl solution. The impedance spectra for the Nyquist plot shown in Fig. 4a were analyzed by fitting it to the equivalent circuit model shown in Fig. 5a. The parameters obtained by fitting the equivalent circuit and the values of the passivation efficiency (PE%) are listed in Table 2. According to usual convention, R_S represents the solution resistance, Q the constant phase elements (CPEs), R_{P1} the polarization resistance, R_{P2} another polarization

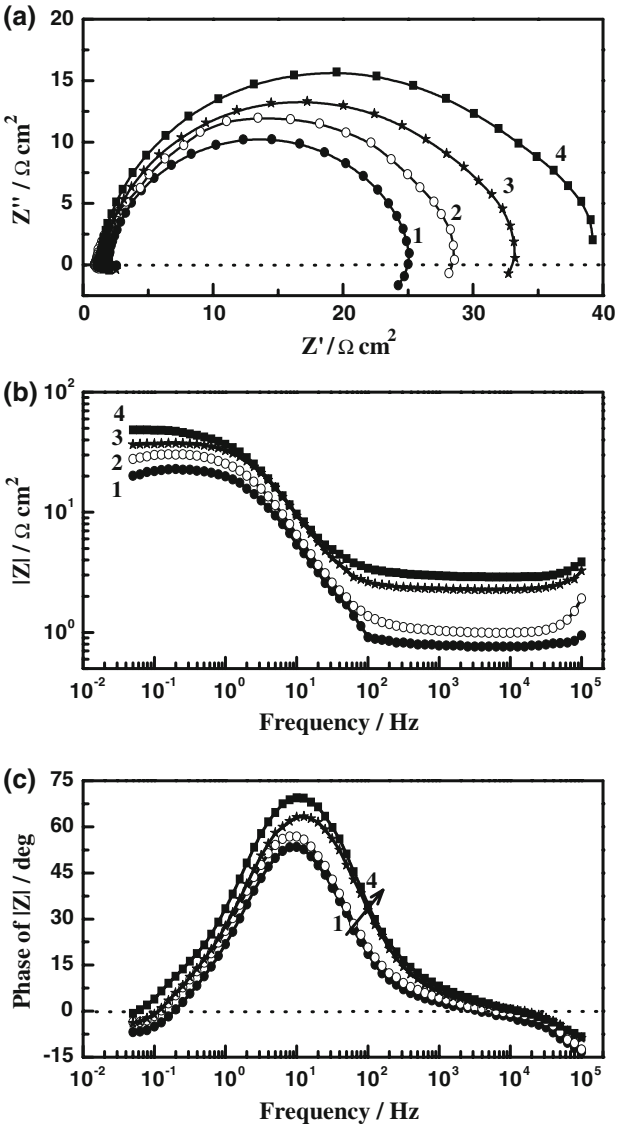

Fig. 4 Typical Nyquist (**a**), Bode (**b**) and phase angle (**c**) plots obtained for DSS alloy I (1), alloy II (2), alloy III (3), and alloy IV (4) after 1 h immersion in 2 M HCl solution

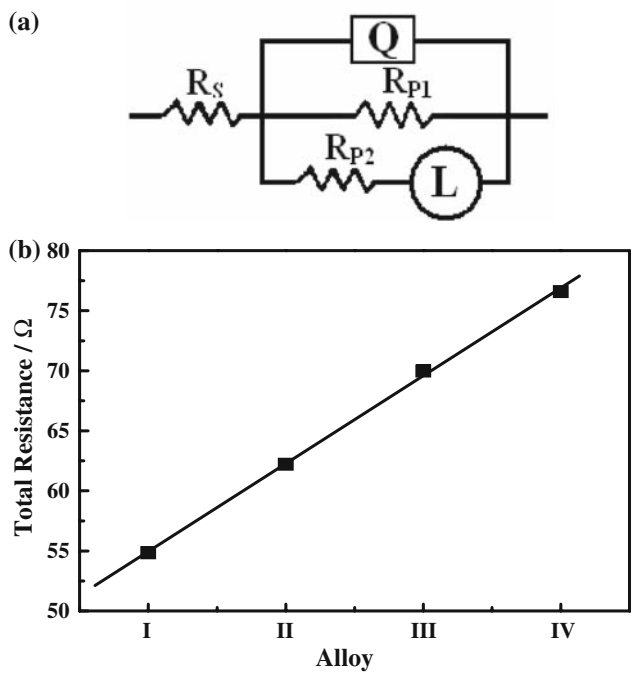

Fig. 5 **a** The equivalent circuit model used to fit the experimental data presented in Fig. 4a; and **b** total polarization resistances plotted as a function of the DSS alloy number

resistance, and L the conductance. It is clear from Fig. 4a that only single but distorted semicircles are observed for the DSS electrode regardless of whether Ru is present or not. The presence of Ru linearly raises the total resistance ($R_{P1} + R_{P2}$) for the electron transfer reaction as shown in Fig. 5b. This increase in the resistance of both electron transfer reactions upon increasing the Ru content is in general agreement with the positive shift in the pitting and corrosion potentials [29]. The passive layers covering the electrode surfaces seem fairly dense, although they are porous, as the CPEs (Q) are about the same magnitudes as those of typical double-layer capacitances. The CPEs have characteristics similar to those of capacitors with their n values close to 1.0. The steady decrease of CPEs with an increasing Ru content in the alloys indicates reduced capacitive effects through the covering of the charged surfaces [30, 31]. The presence of the inductive (L) loop suggests that the passivated surface re-dissolves at low frequencies [25]. The steady decrease of L values indicates that the dissolution of the passive film formed on the DSS alloys decreases with increasing Ru additions. The semicircles at high frequencies in Fig. 4a are generally associated with the relaxation of electrical double layer capacitors and the diameters of the high frequency semicircles can be considered as the charge transfer resistance (R_{P1}) [32]. Therefore, the values of PE% for the DSS electrode by Ru can be calculated from the charge transfer resistance as follows [17, 18]:

$$\mathrm{PE}\% = \frac{R_{P1} - R_{P1}^{-}}{R_{P1}} \times 100 \quad (4)$$

where R_{P1} and R_{P1}^{-} are the charge-transfer resistances of the DSS alloy with and without Ru, respectively. The increase of PE% with the presence of Ru and its increasing content was also confirmed by the increase of the impedance of the interface (Fig. 4b) and the maximum phase angle (Fig. 4c), which both indicate passivation of the DSS alloy surface.

3.5 Weight-loss measurements

Figure 6 shows the calculated corrosion rate [K_{Corr} (mg dm^{-2} day^{-1}, mdd)] from weight-loss data [33] as a function of time (6–48 h) for the DSS coupons in 100 mL of 2 M HCl. The values of K_{Corr} over the exposure time were calculated as previously reported [16]. It can be seen from Fig. 6 that the value of K_{Corr} increased with time for alloy I due to the chloride ion attack. This attack leads to the dissolution of the DSS alloy as stated in Eq. (1) and indicates the continued corrosion of the alloy with time even if it forms some corrosion products on its surface. These corrosion products are not compact enough and only produce partial protection if it stays on the alloy surface, as is also indicated by the OCP measurements. The presence of 0.14% Ru (alloy II) considerably reduced the aggressiveness of the chloride solution attack on the alloy surface

Table 2 EIS parameters obtained by fitting the Nyquist plot shown in Fig. 4a with the equivalent circuit shown in Fig. 5a for DSS alloys in 2 M HCl solution

Alloy	Parameter						
	R_s (Ω cm^2)	Q		R_{P1} (Ω cm^2)	R_{P2} (Ω cm^2)	L (H)	PE (%)
		Y_Q (F cm^{-2})	n				
I	0.90	0.004825	0.92	22.18	32.67	273.30	–
II	0.95	0.004107	0.92	29.57	33.15	97.99	26.00
III	1.23	0.003722	0.91	35.90	34.08	5.60	38.22
IV	1.57	0.003015	0.90	39.55	37.04	0.28	43.92

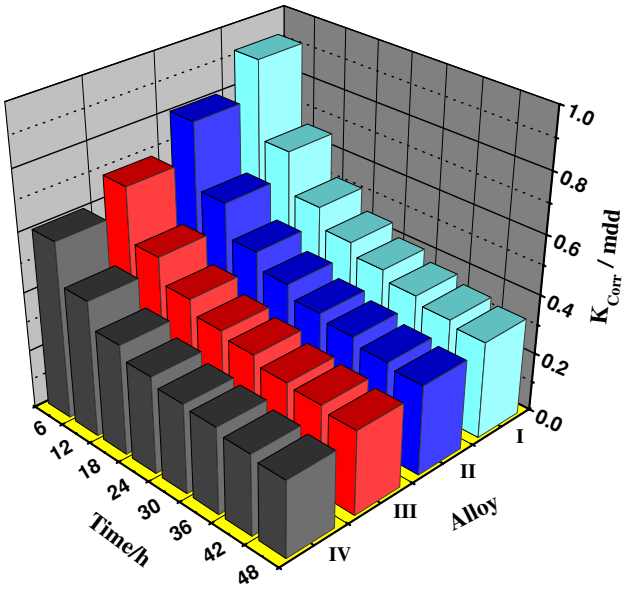

Fig. 6 Change of the corrosion rate (K_{Corr}) versus time for DSS alloys in 2 M HCl solution

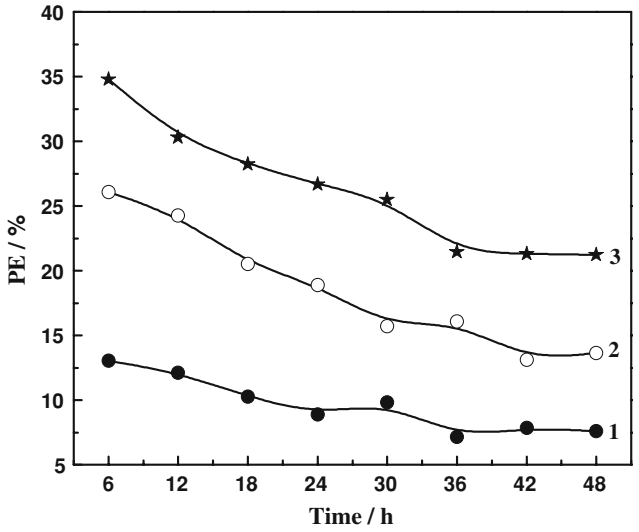

Fig. 7 Variations of PE% versus time for DSS alloy by (1) 0.14%, (2) 0.22%, and (3) 0.28% Ru in 2 M HCl solution

and significantly decreased the increase of K_{Corr} with time. This effect was further enhanced with the increase of the Ru contents to 0.22% (alloy III) and 0.28% (alloy IV).

Moreover, the values of the passivation efficiency (PE%) of the DSS by Ru were also calculated using the following equation [15, 17];

$$PE\% = \frac{K^1_{Corr} - K^2_{Corr}}{K^1_{Corr}} \times 100 \quad (5)$$

where K^1_{Corr} and K^2_{Corr} are the corrosion rates (mdd) for the DSS alloy in the absence and presence of Ru, respectively. The variation of PE% versus time for the DSS alloy by 0.14% (1), 0.22% (2), and 0.28% Ru (3) in the test solution is shown in Fig. 7. The maximum passivation of DSS by Ru is obtained by increasing the Ru content and decreasing the immersion time of the alloy in the chloride solution.

4 Conclusions

The effects of 0.14%, 0.22%, and 0.28% Ru additions on the passivation of DSS corrosion in 2 M HCl solution have been investigated using a variety of electrochemical and gravimetric measurements. OCP measurements showed significant positive shifts towards more noble values in the corrosion potential as a result of the presence of Ru in the alloy. Polarization experiments revealed a considerable reduction in the corrosion rate parameters due to the presence of an increasing Ru content. Potentiostatic current–time measurements at −100, −50, and 50 mV and EIS experiments indicated that the increased addition of Ru is a powerful driving force to decrease the pitting and anodic dissolutions of DSS through increasing its surface and polarization resistances, its interface impedance, and its maximum phase angle. Weight-loss data confirmed that the presence of Ru greatly decreases the weight-loss and corrosion rate, while increasing the passivation efficiency of the alloy. This effect increases with increasing Ru contents and decreasing immersion times. The results from the combined measurements agree well with one another and prove beyond doubt that the presence of Ru, and an increasing amount thereof, greatly enhances the corrosion resistance of protect the DSS alloys against general and pitting corrosion in the 2 M HCl solution.

Acknowledgements This research work was supported by the DST/NRF Centre of Excellence in Strong Materials, who also awarded a Postdoctoral Fellowship to EMS.

References

1. Potgieter JH, Olubambi PA, Cornish L, Machio CN, Sherif EM (2008) Corros Sci 50:2572
2. Varga K, Baradlai P, Barnard WO, Myburg G, Halmos P, Potgieter JH (1997) Electrochim Acta 42:25
3. Potgieter JH (1991) J Appl Electrochem 21:471
4. Potgieter JH, Heyns AM, Skinner W (1990) J Appl Electrochem 20:711
5. Baradlai P, Potgieter JH, Barnard WO, Tomcsanyi L, Varga K (1995) Mater Sci Forum 185–188:759
6. Myburg G, Varga K, Barnard WO, Baradlai P, Tomcsânyi L, Potgieter JH, Louw CW, Van Staden MJ (1998) Appl Surf Sci 136:29
7. Potgieter JH, Barnard WO, Myburg G, Varga K, Baradlai P, Tomcsânyi L (1996) J Appl Electrochem 26:1103
8. Potgieter JH, Skinner W, Heyns AM (1993) J Appl Electrochem 23:11
9. Tjong SC (1990) Appl Surf Sci 44:7

10. Wolff IM, Iorio LE, Rumpf T, Scheers PVT, Potgieter JH (1998) Mater Sci Eng A 241:264
11. Potgieter JH, Ellis P, Van Bennekom A (1995) ISIJ Int 35:197
12. Sherif EM, Park SM (2006) Corros Sci 48:4065
13. Sherif EM (2006) Appl Surf Sci 252:8615
14. Sherif EM, Park SM (2006) Electrochim Acta 51:4665
15. Sherif EM, El Shamy AM, Ramla MM, El-Nazhawy AOH (2007) Mater Chem Phys 102:231
16. Sherif EM, Erasmus RM, Comins JD (2009) J Appl Electrochem 39:83
17. Sherif EM, Park SM (2005) J Electrochem Soc 152:B428
18. Sherif EM, Park SM (2006) Electrochim Acta 51:6556
19. Van Staden MJ, Roux JP (1990) Appl Surf Sci 44:263
20. Tjong SC, Barnard WO, Malherbe JB (1992) J Mater Sci 27:1818
21. Szklarska-Smialowska Z (1986) Pitting corrosion of metals. NACE, Huston
22. Park SM, Yoo JS (2003) J Anal Chem 75:455A
23. Macdonald JR (1987) Impedance spectroscopy. Wiley, New York
24. Sherif EM, Erasmus RM, Comins JD (2007) J Colloid Interface Sci 309:470
25. Sherif EM, Park SM (2006) Electrochim Acta 51:1313
26. Sherif EM, Park SM (2005) J Electrochem Soc 152:B205
27. Sherif EM, Erasmus RM, Comins JD (2007) J Colloid Interface Sci 311:144
28. Sherif EM, Erasmus RM, Comins JD (2007) J Colloid Interface Sci 306:96
29. Mansfeld F, Lin S, Kim S, Shih H (2007) Corros Sci 27:997
30. Larabi L, Harek Y, Benali O, Ghalem S (2005) Prog Org Coat 54:256
31. Popova A, Sokolova E, Raicheva S, Christov M (2003) Corros Sci 45:33
32. Ma H, Chen S, Niu L, Zhao S, Li S, Li D (2002) J Appl Electrochem 32:65
33. Sherif EM, Erasmus RM, Comins JD (2008) Corros Sci 50:3439